ELSEVIER

Journal of Molecular Catalysis A: Chemical 159 (2000) 233–245

JOURNAL OF MOLECULAR CATALYSIS A: CHEMICAL

www.elsevier.com/locate/molcata

Stability and reactivity of low-spin ferric hydroperoxo and alkylperoxo complexes with bipyridine and phenantroline ligands

A.P. Sobolev [a], D.E. Babushkin [b], E.P. Talsi [b,*]

[a] *Department of Natural Sciences, Novosibirsk State University, Novosibirsk 630090, Russia*
[b] *Boreskov Institute of Catalysis, Pr. Akademika Lavrentieva 5, Novosibirsk 630090, Russia*

Received 1 May 1999; received in revised form 14 February 2000; accepted 28 February 2000

Abstract

In this work the first-order rate constants of self-decomposition of hydroperoxo and alkylperoxo complexes $[Fe(bpy)_2(OOH)Py](NO_3)_2$ (**2a**-Py), $[Fe(phen)_2(OOH)Py](NO_3)_2$ (**2b**-Py) and $[Fe(bpy)_2(OOtBu)CH_3CN](NO_3)_2$ (**3a**-CH_3CN) were determined in the presence of various substrates and at various temperatures. It was observed, that the alkylperoxo species are far less stable than corresponding hydroperoxo intermediates, $k = 1.2 \times 10^{-2}$ s^{-1} (**3a**-CH_3CN in CH_3CN at -10°C) and $k = 2 \times 10^{-4}$ s^{-1} (**2a**-Py in CH_3CN at -10°C). The sixth ligand (Py in **2a**-Py and **2b**-Py; CH_3CN in **3a**-CH_3CN) can be replaced by other donor molecules B in appropriate solvent systems. Using d_9-*t*BuOOH, ^{2}D NMR signals of *t*BuOO moieties of complexes **3a**-CH_3CN, **3a**-CH_3OH and **3a**-H_2O were observed. The rate of decomposition of hydroperoxo complexes $[Fe(bpy)_2(OOH)B](NO_3)_2$ (**2a**-B), where B are derivatives of Py (3-Br-Py, 3-Me-Py, 4-Me-Py and 4-Me_2N-Py) increases with the growth of basisity of B (push effect). Such effect is markedly smaller for alkylperoxo species $[Fe(bpy)_2(OOtBu)B](NO_3)_2$ (**3a**-B). The addition of organic substrates (cyclohexane, cyclohexene, methyl phenyl sulfide) in concentrations up to 3 M at -10°C to $+20$°C does not noticeably change the rate of self-decomposition of **2a**-B, $[Fe(phen)_2(OOH)B](NO_3)_2$ (**2b**-B) and **3a**-B. Thus the intermediates concerned do not directly react with organic substrates. The reactivity patterns of **2a**-B, **2b**-B and **3a**-B were characteristic for free radical oxidation. $OH^{\cdot}$ and $HO_2^{\cdot}$ radicals were trapped in solution containing **2a**-Py, and *t*BuOO$^{\cdot}$ free radicals were detected in solution in the presence of **3a**-B. The determined rates of self-decomposition of complexes **2a**-B, **2b**-B and **3a**-B can be used for evaluation of the upper limit for their reactivity towards organic substrates.

Keywords: Ferric hydroperoxo complexes; Ferric alkylperoxo complexes; EPR; NMR spectroscopy; Reactivity studies

1. Introduction

There have been several efforts aimed at modelling of the alkane functionalization chemistry of nonheme iron enzymes; most prominent of these are the catalysts known as the ''Gif'' systems [1–3], $[Fe_2O(bpy)_4]^{4+}/t$BuOOH [4] and $[Fe(TPA)Cl]^{2+}/t$BuOOH [5,6] combinations (TPA — tris(2-pyridylmethyl)amine).

Two alternative mechanisms of alkane oxidation by these catalytic systems are supposed now in the literature. According to one of them,

* Corresponding author. Tel.: +7-383-234-1877; fax: +7-383-234-3056.
E-mail address: talsi@catalysis.nsk.su (E.P. Talsi).

1381-1169/00/$ - see front matter
PII: S1381-1169(00)00197-7

metal based oxidant, either a metal-peroxide intermediate or a high-valent iron-oxo species derived therefrom, must participate in the alkane functionalization reactions [1–5]. According to the other, alkylperoxy or alkoxy radicals are supposed to be reactive intermediates [7–10].

Since high-valent iron-oxo intermediates have never been observed spectroscopically for non-heme catalytic systems, the assumption that ferric-hydroperoxide could be itself a highly reactive species is rather spread in the literature (see Refs. [11–13]). Nevertheless, this possibility requires much more experimental and theoretical studies.

During the last 5 years, molecular composition of several low-spin alkylperoxo and hydroperoxo iron intermediates [Fe(BLM)(OOH)] (activated bleomycin) [14–16], $[Fe^{III}(bpy)_2(OOtBu)HOR]^{2+}$ [17], $[Fe^{III}(TPA)(OOtBu)(HOR)]^{2+}$ [18], $[Fe^{III}(N4Py)(OOH)]^{2+}$ (where N4Py is *N*-(bis(2-pyridyl)-methyl)-*N*,*N*-bis(2-pyridylmethyl)amine) [19], $[Fe^{III}(Py5)(OOH)]^{2+}$ (where Py5 is 2,6-bis-(bis(2-pyridyl) methoxymethane)pyridine) [20] and $[Fe^{III}(TPA)(OOH)]^{2+}$ [21,22] has been reliably determined using EPR, resonance Raman and electrospray ionization mass spectroscopies. Some intermediates $[Fe^{III}(TPP)(OOH)(OH)]$ [23], $[Fe^{III}(cyclyd)(OOH)]$ [24], $[Fe^{III}(F_{20}TPP)(OOC(O)Ar)]$ [25], $[Fe^{III}(PMA)(OOH)]$ and $[Fe^{III}(PMA)(OOtBu)]$ [26,27], $[Fe(bpy)_2(OOH)Py](NO_3)_2$ and $[Fe(phen)_2(OOH)Py](NO_3)_2$ [28] have been characterized by EPR spectroscopy based on their highly characteristic anisotropy of *g*-tensor.

However in all cases, except activated bleomycin Fe(BLM)(OOH) [14,15], the reactivity data were insufficient to evaluate the impact of these intermediates to the oxidation of organic substrates.

In this work we describe our detailed studies of the stability and reactivity of ferric hydroperoxo and alkylperoxo complexes $[Fe(bpy)_2(OOH)Py](NO_3)_2$ (**2a**-Py), $[Fe(phen)_2(OOH)Py](NO_3)_2$ (**2b**-Py) and $[Fe(bpy)_2(OOtBu)CH_3CN](NO_3)_2$ (**3a**-CH_3CN). These complexes were previously found in the reaction of HOOH with $[Fe_2O(bpy)_4 \cdot 2H_2O](NO_3)_4$ (**1a**) and $[Fe_2O(phen)_4 \cdot 2H_2O](NO_3)_4$ (**1b**) in Py/AcOH mixture as a solvent [28], and in the reaction of *t*BuOOH with **1a** in ROH/CH_3CN mixture [17].

2. Experimental part

2.1. Materials

Cyclohexane, methyl phenyl sulfide, pyridine, 3-Me–, 4-Me–, 3-Br–, 2-Me–, 4-dimethylamino pyridines, glacial acetic acid, acetonitrile, methanol and corresponding deuterated solvents were purchased from Aldrich and used without additional purification. Purchased cyclohexene was purified by double fractional distillation just before using. Hydrogen peroxide 30% was concentrated in vacuum up to 90–95% and titrated with $KMnO_4$ just before experiments. *Tert*-butyl hydroperoxide and deuterated *tert*-butyl hydroperoxide (d_9-*t*BuOOH) were obtained from *tert*-butyl alcohol and deuterated *tert*-butyl alcohol (d_9-*t*BuOH) according to procedure described in Refs. [29,30]. Complexes **1a** and **1b** were prepared as described in Refs. [31,32], respectively.

2.2. EPR monitoring of hydroperoxo complex *2a*-Py in the catalytic system *1a*/HOOH/AcOH/Py

To start the reaction, 0.2 ml of 0.01 M solution of complex **1a** in 2:1 Py/AcOH molar mixture or in this mixture containing cyclohexane was added to (frozen in liquid nitrogen) 0.02 ml of 90% HOOH (370 equiv.) directly in an EPR tube. Then the sample was immersed in a constant-temperature bath with water and solutions of **1a** and HOOH were mixed. To stop the reaction, the EPR tube was immersed in liquid nitrogen followed by registration of EPR

spectrum at −196°C. Thus, dependencies of **2a**-Py concentration versus time were obtained.

2.3. Preparation of the solutions of *2a*-Py, *2b*-Py and *3a*-CH_3CN with reduced concentration of peroxides

A mixture of 0.6 ml of 1:1 Py/90% HOOH volume was added dropwise into 1 ml of 0.01 M solution of complex **1a** or **1b** in 2:1 Py/AcOH molar mixture at −20°C (catalyst:oxidant ratio = 1:1100 equiv.). The sample was warmed up to 0°C and kept 5–10 min at this temperature to rich 10^{-3} M concentration of **2a**-Py or **2b**-Py. Then the solution was mixed with 20 ml of diethyl ether at −60°C and kept 30–40 min at this temperature to obtain precipitate, containing **2a**-Py or **2b**-Py as an admixture. After that, the liquid part was decanted and the precipitate was again washed with 20 ml of diethyl ether at −60°C. The washing procedure was repeated three times and then residual diethyl ether was removed under vacuum. The residue was dissolved in appropriate solvent system at low temperature to give solutions of $[Fe(bpy)_2(OOH)B](NO_3)_2$ (**2a**-B) or $[Fe(phen)_2(OOH)B](NO_3)_2$ (**2b**-B) with the reduced concentration of HOOH. Concentration of residual HOOH (monitored by iodometric titration) was less than 10^{-2} M and that of **2a**-B or **2b**-B (monitored by EPR) was about 2×10^{-4} M. To study the interaction with organic substrates, the solution containing **2a**-Py or **2b**-Py was sampled into several EPR tubes at low temperature. Some of these tubes contained the appropriate amount of a substrate. The reaction was started by immersing all tubes into a constant-temperature bath with ethyl alcohol. The solutions in EPR tubes were thoroughly mixed. The reaction was stopped by simultaneously freezing all the samples in liquid nitrogen. Then EPR spectra of hydroperoxo intermediates were recorded at −196°C. The reaction was started again by immersing all the tubes in the bath. Thus obtained kinetic curves for complexes **2a**-Py or **2b**-Py decomposition in the presence and in the absence of various substrates can be reliably compared.

The procedure used for preparation of **3a**-CH_3CN samples with reduced concentration of *t*BuOOH was similar to that described above. In this case, the interaction of **1a** ([**1a**] = 0.01 M) with 500 equiv. of *t*BuOOH was performed in 1:4 MeOH/CH_3CN molar mixture at −40°C. The characteristic green color indicated formation of **3a**-CH_3CN. Solid samples containing **3a**-CH_3CN were isolated by the same procedure as in the case of **2a**-Py.

2.4. EPR measurements

EPR spectra (−196°C) were recorded at 9.2–9.3 GHz on a Bruker ER-200D spectrometer in glass cylindrical tubes (d = 5 mm). They were simulated using an extended version of the EPR 1 program, described in Ref. [33]. Measurements were made in a quartz Dewar with liquid nitrogen. The dual EPR cavity furnished with the spectrometer was used. Periclase crystal (MgO), with impurities of Mn^{2+} and Cr^{3+}, served as a side reference, was placed into the center of the second compartment of the dual cavity. EPR signals were quantified by double integration with copper chloride as a standard at −196°C. A flat quartz cell was used for registration of EPR spectra of liquid samples at room temperature.

2.5. NMR measurements

^{2}D NMR spectra were recorded at 61.40 MHz in 10-mm glass sample tubes, using pulsed FT-NMR technique, with a Bruker MSL-400 NMR spectrometer. The typical operating conditions used for ^{2}D NMR measurements were as follows: sweep width 3 kHz; spectrum accumulation frequency 2.5 Hz; number of transients 5000–10 000; 45° pulse at 10 μs. ^{1}H NMR spectra were monitored on the Bruker MSL-400 NMR spectrometer at 400.13 MHz and a Bruker DPX-250 NMR instrument at 250.10 MHz as well.

2.6. The analysis of the oxidation products

The yield of the reaction products (cyclohexanone, cyclohexanol, cyclohexenone and cyclohexenol) was measured using GC technique (chromatograph ''Tsvet 500'', FID, Ar, a steel column (2 m × 3 mm) packed with 15% Carbowax 20M on Chromaton N-AW-HMDS). Probes (0.5 ml) of the reaction solutions were sampled, followed by the extraction of the reaction products with diethyl ether (3 × 1 ml). The diethyl ether layers were combined; styrene was added as an internal standard. Diethyl ether was evaporated and the mixture was analyzed by GC. Products were identified and quantitated by comparison with authentic samples.

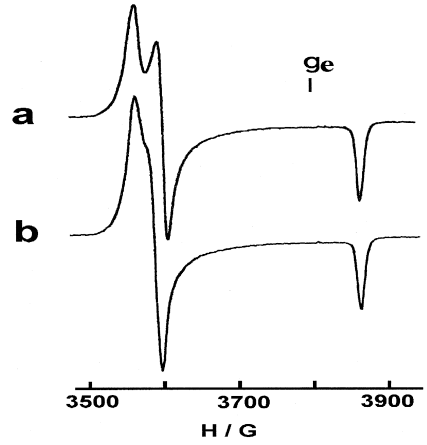

Fig. 1. X-band EPR spectra of complexes **2a**-Py (a) and **2b**-Py (b) at −196°C in 2:1 pyridine/AcOH molar mixture. Spectrometer settings: microwave power 20 mW, modulation frequency 100 kHz, modulation amplitude 5 G.

3. Results and discussion

3.1. Characterization of hydroperoxo complexes *2a*-*B* and *2b*-*B*

The intensities of the EPR signals of complexes $[Fe(bpy)_2(OOH)Py](NO_3)_2$ (**2a**-Py) and $[Fe(phen)_2(OOH)Py](NO_3)_2$ (**2b**-Py) (Fig. 1a and b) correspond to their yield as much as 20% based on starting complexes **1a** or **1b**. The *g*-values of complexes **2a**-Py (2.14, 2.11, 1.97) and **2b**-Py (2.13, 2.12, 1.97) were rather close to those for recently well characterized hydroperoxo complexes $[Fe^{III}(N4Py)(OOH)]^{2+}$ (2.17, 2.12, 1.98) [19], $[Fe^{III}(Py5)(OOH)]^{2+}$ (2.15, 2.13, 1.98) [20] and $[Fe^{III}(TPA)(OOH)]^{2+}$ (2.19, 2.14, 1.97) [21]. The typical *g*-values for stable low-spin ferric complexes with O,N-donor ligands containing no OOH or OOR moieties are in the range $g_1 = 2.4–2.6$, $g_2 = 2.14–2.2$, $g_3 = 1.85–1.95$ [34,35]. The observed low anisotropy of *g*-factors for the complexes **2a**-Py and **2b**-Py is a highly characteristic property of low-spin ferric hydroperoxo or alkylperoxo species. The attempts to characterize **2a**-Py and **2b**-Py by electrospray ionization mass spectrometry were unsuccessful. However, it is unlikely that the supposed molecular composition of the complexes **2a**-Py and **2b**-Py will be essentially refined. Indeed, their monomeric structure is evident from EPR spectra typical of a mononuclear low-spin iron(III) center in an octahedral environment. The presence of at least two bipyridine or phenantroline ligands is necessary to obtain low-spin ferric species, the presence of the hydroperoxo moiety is evident from the characteristic anisotropy of g-tensor. Low-spin ferric complexes must be six-coordinated. This sixth ligand is pyridine.

A sample of **2a**-Py obtained after extraction of HOOH from the reaction mixture and removal of the major part of Py/AcOH (the residual concentration of HOOH was ca. 10^{-2} M and that of AcOH or Py was also not more than 10^{-2} M, see Section 2) was dissolved in CH_3CN. The EPR spectrum of this new sample only slightly differs from that of **2a**-Py. Thus, the replacement of Py in **2a**-Py by CH_3CN does not occur, otherwise it should lead to noticeable changes in EPR spectral parameters as in the case of related complexes $[Fe(bpy)_2(OOtBu)B](NO_3)_2$ **3a**-B. Their EPR spectra are very sensitive to the nature of the sixth ligand (CH_3CN or Py, see Table 1). The *g*-values of **2a**-Py change insignificantly when Py is replaced by its derivatives B with various pK_a

Table 1
EPR spectroscopic data for low-spin ferric peroxo and alkylperoxo complexes

Complex	Solvent	g_1	g_2	g_3	Ref.
$[Fe(N4Py)(OOH)]^{2+}$	CH_3CN	2.17	2.12	1.97	[19][a]
$[Fe(Py5)(OOH)]^{2+}$	CH_3CN	2.15	2.13	1.98	[20][b]
$[Fe(TPA)(OOH)]^{2+}$	CH_3CN	2.19	2.14	1.97	[21][c]
$[Fe(bpy)_2(OOH)Py]^{2+}$, **2a**-Py	Py/AcOH	2.14	2.11	1.97	[28]
$[Fe(bpy)_2(OOH)Py]^{2+}$, **2a**-Py	CH_3CN/Py	2.14	2.11	1.97	this work
$[Fe(phen)_2(OOH)Py]^{2+}$, **2b**-Py	Py/AcOH	2.13	2.12	1.97	[28]
$[Fe(4,4'\text{-}Me_2\text{-}bpy)_2(OOH)Py]^{2+}$	CH_3CN/Py	2.14	2.11	1.97	this work
$[Fe(bpy)_2(OO\,t\text{Bu})CH_3CN]^{2+}$, **3a**-$CH_3CN$	CH_3CN	2.18	2.12	1.98	this work
$[Fe(bpy)_2(OO\,t\text{Bu})MeOH]^{2+}$, **3a**-MeOH	MeOH	2.18	2.16	1.98	this work
$[Fe(bpy)_2(OO\,t\text{Bu})H_2O]^{2+}$, **3a**-$H_2O$	CH_3CN	2.18	2.16	1.98	this work
$[Fe(bpy)_2(OO\,t\text{Bu})Py]^{2+}$, **3a**-Py	CH_3CN/Py	2.18	2.13	1.975	this work
$[Fe(bpy)_2(OO\,t\text{Bu})(3\text{-Br-Py})]^{2+}$, **3a**-3-Br-Py	CH_3CN/3-Br-Py	2.18	2.13	1.975	this work
$[Fe(phen)_2(OO\,t\text{Bu})CH_3CN]^{2+}$, **3b**-$CH_3CN$	CH_3CN	2.16	2.10	1.97	this work

[a] N4Py = *N*-(bis(2-pyridyl)-methyl)-*N*,*N*-bis(2-pyridylmethyl)amine.
[b] Py5 = 2,6-bis-(bis(2-pyridyl)methoxymethane)pyridine.
[c] TPA = tris-(2-pyridylmethyl)amine.

(3-Br-Py, 3-Me-Py, 4-Me-Py or 4-Me_2N-Py). This replacement can be readily performed by the addition of B at a concentration of 1 M to a sample of **2a**-Py in CH_3CN (residual concentration of Py was less than 10^{-2} M).

*3.2. Characterization of alkylperoxo complexes **3a**-B*

Recently, alkylperoxo complexes with supposed structure $[Fe(bpy)_2(OO\,t\text{Bu})ROH](ClO_4)_2$ (**3a**-ROH), where ROH = benzyl alcohol, methanol and phenol, were detected by EPR in the reaction of **1a** with *t*BuOOH in CH_3CN/ROH mixtures. The presence of OO*t*Bu moiety in **3a**-ROH was confirmed by resonance Raman spectroscopy [17]. However, the EPR signal ($g = 2.18$, 2.12, 1.98) attributed in Ref. [17] to **3a**-ROH belongs in fact to complex **3a**-CH_3CN with CH_3CN molecule on the sixth coordination site (Fig. 2c). Complex **3a**-MeOH ($g = 2.18$, 2.16, 1.98) can be obtained in neat methanol (Fig. 2a), while in methanol/acetonitrile mixtures the complexes **3a**-MeOH and **3a**-CH_3CN both are present (Fig. 2b). Complexes **3a**-B (B is a donor molecule) can be prepared by dissolution of a sample, containing **3a**-CH_3CN in CH_3CN/B solvent system at −40°C. EPR parameters of complexes **3a**-B are presented in Table 1. It is seen that *g*-factors for complexes **3a**-MeOH and **3a**-H_2O are close.

Further ^{2}D NMR spectroscopic studies provide new insight into the structures of the **3a**-B intermediates, formed in the reaction of **1a** with *t*BuOOH in CH_3CN/MeOH mixtures. When deuterated d_9-*t*BuOOH was added to the solution of **1a** in 1:3 MeOH/CH_3CN molar mixture at −35°C, two weak resonances at −3.1 and at −3.7 ppm along with an intense signal of d_9-

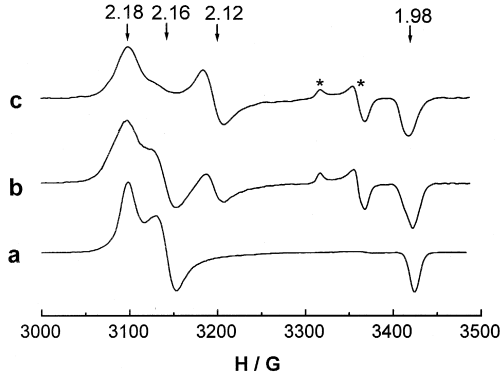

Fig. 2. X-band EPR spectra of complexes **3a**-MeOH and **3a**-CH_3CN formed in the reaction of **1a** (5×10^{-3} M) with 200 equiv. of *t*BuOOH at −35°C in various MeOH/CH_3CN molar mixtures: (a) in neat MeOH; (b) 1:1 MeOH/CH_3CN; (c) 1:40 MeOH/CH_3CN. The spectra were recorded at −196°C. The signal denoted by asterisks belongs to *t*BuOO$^{\cdot}$ radical.

*t*BuOOH and d_9-*t*BuOH at 1.22 ppm were observed in the ^{2}D NMR spectrum (Fig. 3a). The intensities of these resonances correlated with the intensities of the EPR signals for the complexes **3a**-MeOH and **3a**-CH_3CN detected in the same sample. The signals at -3.1 and -3.7 ppm can be ascribed to the alkylperoxo moieties of **3a**-MeOH and **3a**-CH_3CN respectively. The ratio of their intensities in ^{2}D NMR spectra was proportional to that of MeOH and CH_3CN concentrations. Addition of water to the reaction mixture afforded a new signal at -2.5 ppm attributed to the *t*BuOO group of **3a**-H_2O (Fig. 3b). The intensity of the particular resonance was found to be proportional to the concentration of the corresponding ligand (MeOH, CH_3CN or H_2O) in solution. It implies the occurrence of equilibria between the complexes **3a**-MeOH, **3a**-CH_3CN and **3a**-H_2O, as shown in Eqs. (1)–(3)

$$\textbf{3a}\text{-MeOH} + CH_3CN \overset{K_1}{\rightleftarrows} \textbf{3a}\text{-}CH_3CN + MeOH \quad (1)$$

$$\textbf{3a}\text{-MeOH} + H_2O \overset{K_2}{\rightleftarrows} \textbf{3a}\text{-}H_2O + MeOH \quad (2)$$

$$\textbf{3a}\text{-}CH_3CN + H_2O \overset{K_3}{\rightleftarrows} \textbf{3a}\text{-}H_2O + CH_3CN \quad (3)$$

According to EPR data the time of establishing of these equilibria was 5–10 min at -35°C. The equilibrium constants K_1–K_3 determined from ^{2}D NMR spectra (at -35°C) have the following values: $K_1 = 0.5 \pm 0.1$; $K_2 = 8 \pm 1$; $K_3 = 16 \pm 2$. It is noteworthy that the substitution of MeOH by H_2O molecule on the sixth coordination site of **3a**-MeOH gives rise to noticeable change in the chemical shift of the alkylperoxo moiety while the difference between EPR parameters of **3a**-MeOH and **3a**-H_2O is negligible. The NMR spectra of Fig. 3 is the first example of the NMR detection of the alkylperoxo moiety for low-spin ferric alkylperoxo species. The reported chemical shifts for α and β deuterium atoms of $OOCD_2CD_3$ group in the high-spin alkylperoxo complex Fe(TPP)($OOCD_2CD_3$) were 180 and 4 ppm, respectively [36]. The ^{1}H NMR resonances of bipyridine ligands of complexes **3a**-B were either too broad to be observed or masked by signals of the initial complex **1a** and by those of undeuterated admixtures in the solvent and peroxide used.

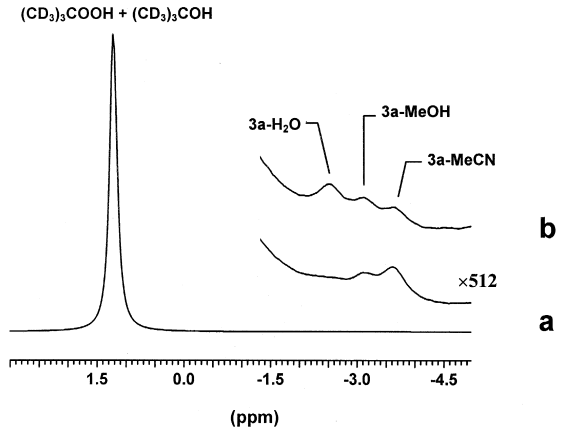

Fig. 3. ^{2}D NMR spectra recorded in the course of the reaction of **1a** ([**1a**] = 0.01 M) with 100 equiv. of d_9-*t*BuOOH at -35°C (a) in 1:3 MeOH/CH_3CN molar mixture; (b) in 1:1.5 MeOH/CH_3CN molar mixture, where H_2O ([H_2O] = 1 M) was added.

*3.3. Stability of hydroperoxo complexes **2a**-B and **2b**-B*

First of all, let us consider the results of EPR monitoring of the hydroperoxo intermediate **2a**-Py in the catalytic system **1a**/HOOH/Py/AcOH. Fig. 4a shows the time-dependence of the **2a**-Py concentration in the course of the reaction of **1a** with HOOH at 20°C in 2:1 Py/AcOH mixture ([**1a**] = 0.01 M, [HOOH] = 3 M). It is seen that the concentration of complex **2a**-Py reached maximum during 3 h, was in steady state for 1 h, and then decreased by a pseudo-first-order kinetics with the rate constant $(3 \pm 1) \times 10^{-4}$ s^{-1}.

The steady-state concentration of **2a**-Py dropped 5 ± 0.5 times if C_6H_{12} ([C_6H_{12}] = 1 M) had been previously added to a sample (Fig. 4b). The value of this drop depended on the cyclohexane concentration and was 3 ± 0.6 at

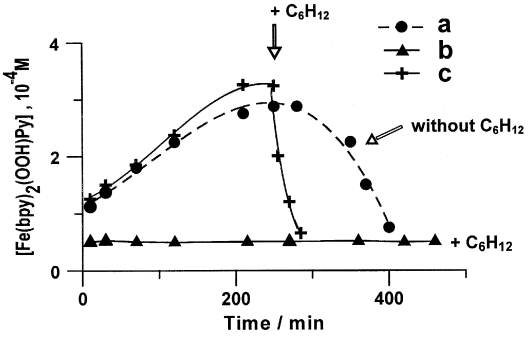

Fig. 4. Concentration of **2a**-Py as a function of time in the reaction of **1a** ([**1a**] = 0.01 M) with 90% HOOH ($[HOOH]_0 = 3$ M) at 20°C in 2:1 Py/AcOH (a) and in this mixture, containing C_6H_{12} (1 M) (b). The sample in (a), if C_6H_{12} ($[C_6H_{12}] = 1$ M), was added 4 h after the reaction beginning (c). The difference between curves (a) and (c) before addition of C_6H_{12} shows the level of reproducibility of the samples.

$[C_6H_{12}] = 0.5$ M and 2 ± 0.4 at $[C_6H_{12}] = 0.25$ M.

The addition of cyclohexane ($[C_6H_{12}] = 1$ M) to the sample of Fig. 4a at a moment when the steady-state concentration of **2a**-Py had already been established, gave rise to the rapid decrease of the concentration of **2a**-Py down to the value corresponding to the presence of cyclohexane in solution initially (Fig. 4c). This conversion followed a first-order kinetics with $k = (1.5 \pm 0.5) \times 10^{-3}$ s^{-1}.

The concentration of **2a**-Py is determined by the competition of the rates of its formation (W_1) and decay (W_2). The effect of cyclohexane (Fig. 4c) could result either from decrease of W_1 or increase of W_2. To distinguish between these two possibilities, it is necessary to measure the rate of self-decomposition of **2a**-Py and determine the influence of organic substrates on this rate.

The reasonable way to measure self-decay kinetics of **2a**-Py is to dramatically diminish the concentration of HOOH in the reaction solution at low temperature and thus sharply decrease the rate of **2a**-Py formation. The subsequent monitoring of the decrease of the concentration of **2a**-Py at higher temperatures allows determination of the rate of its self-decomposition. This procedure will give the real value of the rate of **2a**-Py self-decomposition, if the loss of **2a**-Py concentration during the removal of HOOH at low temperature is markedly smaller than the decrease of the concentration of HOOH. The extraction of peroxide from reaction mixture by diethyl ether at low temperature (see Section 2) permits fulfillment of these requirements. The loss of the **2a**-Py concentration during extraction of HOOH (from 2×10^{-3} to 2×10^{-4} M) was markedly smaller than the decrease of HOOH concentration (from 3 to 10^{-2} M). The similar procedure was used for preparation of complexes **2b**-Py and **3a**-CH_3CN. Further, if not especially noted, the data for samples with the reduced concentration of peroxides will be present.

The procedure described above allows us to obtain **2a**-Py, **2b**-Py and **3a**-CH_3CN only as small admixtures (1–3%) to other ferric complexes. According to ^1H NMR data, in the case of **2a**-Py and **2b**-Py, the major part of iron species represents trinuclear basic iron(III) acetate $[Fe_3(\mu_3\text{-}O)(CH_3CO_2)_6Py_3](NO_3)$ formed upon dissolution of the (μ-oxo)diiron(III) complexes $[Fe_2O(bpy)_4 \cdot 2H_2O](NO_3)_4$ and $[Fe_2O(phen)_4 \cdot 2H_2O](NO_3)_4$ in pyridine/acetic acid mixture. Its identity was confirmed by ^1H NMR, using $[Fe_3(\mu_3\text{-}O)(CH_3CO_2)_6Py_3](ClO_4)$ independently prepared as described in Ref. [37]. Complex **3a**-CH_3CN can be obtained as an admixture to the initial complex **1a** $[Fe_2O(bpy)_4 \cdot 2H_2O](NO_3)_4$. Fortunately, all iron species except alkylperoxo and hydroperoxo intermediates display no signals near $g = 2$ and thus the concentration of these intermediates can be readily monitored by EPR. The obtained kinetic data for self-decay of **2a**-B, **2b**-Py and **3a**-B under various conditions are collected in Table 2.

Complex **2a**-Py dissolved in Py or Py/AcOH mixture was stable at −60°C and decayed with a first-order kinetics at higher temperatures (Fig. 5). The rate constants of this decay determined at various temperatures are the same in Py and in 2:1 Py/AcOH mixture and have the following values: $k = 5 \times 10^{-4}$ s^{-1} (−27°C); 1×10^{-3} s^{-1} (−20°C); 2.8×10^{-3} s^{-1}

Table 2
First order rate constants of low-spin ferric hydroperoxo and alkylperoxo complexes self-decay[a]

Complex	Temperature (°C)	Solvent system	$k \times 10^3$ (s^{-1})
$[Fe(bpy)_2(OOH)Py](NO_3)_2$	−27	Py/AcOH[b]	0.5
$[Fe(bpy)_2(OOH)Py](NO_3)_2$	−20	Py/AcOH[b]	1.0
$[Fe(bpy)_2(OOH)Py](NO_3)_2$	−10	Py/AcOH[b]	2.8
$[Fe(bpy)_2(OOH)Py](NO_3)_2$	5	Py/CH_3CN[c]	0.5
$[Fe(bpy)_2(OOH)Py](NO_3)_2$	5	Py/H_2O[c]	2.0
$[Fe(bpy)_2(OOH)(3\text{-Br-Py})](NO_3)_2$	20	$3\text{-Br-Py}/CH_3CN$[d]	0.4
$[Fe(bpy)_2(OOH)Py](NO_3)_2$	20	Py/CH_3CN[c]	2.0
$[Fe(bpy)_2(OOH)(3\text{-Me-Py})](NO_3)_2$	20	$3\text{-Me-Py}/CH_3CN$[e]	2.0
$[Fe(bpy)_2(OOH)(4\text{-Me-Py})](NO_3)_2$	20	$4\text{-Me-Py}/CH_3CN$[f]	2.0
$[Fe(bpy)_2(OOH)(4\text{-}Me_2NPy)](NO_3)_2$	20	$4\text{-}Me_2N\text{-Py}/CH_3CN$[g]	6
$[Fe(4,4'\text{-}Me_2\text{-bpy})_2(OOH)Py](NO_3)_2$	20	Py/CH_3CN[c]	6
$[Fe(phen)_2(OOH)Py](NO_3)_2$	20	Py/CH_3CN[c]	8
$[Fe(bpy)_2(OO\,t\text{Bu})CH_3CN](NO_3)_2$	−37	CH_3CN	1.0
$[Fe(bpy)_2(OO\,t\text{Bu})CH_3CN](NO_3)_2$	−30	CH_3CN	2.5
$[Fe(bpy)_2(OO\,t\text{Bu})CH_3CN](NO_3)_2$	−20	CH_3CN	5.8
$[Fe(bpy)_2(OO\,t\text{Bu})MeOH](NO_3)_2$	−35	MeOH	2.4
$[Fe(bpy)_2(OO\,t\text{Bu})Py](NO_3)_2$	−30	Py/CH_3CN[c]	2.3
$[Fe(bpy)_2(OO\,t\text{Bu})(3\text{-Br-Py})](NO_3)_2$	−30	$3\text{-Br-Py}/CH_3CN$[d]	2.0
$[Fe(bpy)_2(OO\,t\text{Bu})(4\text{-}Me_2N\text{-Py})](NO_3)_2$	−30	$4\text{-}Me_2N\text{-Py}/CH_3CN$[g]	3.0

[a]All of the constants were determined with error less than 20%.
[b]3:1 Py/AcOH volume mixture.
[c][Py] = 1 M.
[d][3-Br-Py] = 1 M.
[e][3-Me-Py] = 1 M.
[f][4-Me-Py] = 1 M.
[g][4-Me_2N-Py] = 1 M.

(−10°C), $E_a = 11.6 \pm 3$ kcal/mol (the initial concentration of **2a**-Py is 10^{-4} to 5×10^{-4} M).

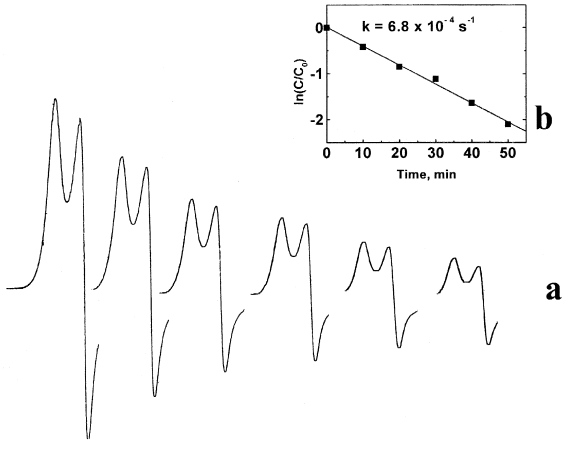

Fig. 5. (a) Low-field part of the EPR signal of complex **2a**-Py in the course of its self-decay in 2:1 Py/AcOH molar mixture at −23°C. The interval between the spectra is 10 min. Inset (b): Plot of the kinetic data from (a) after applying the equation $\ln(C/C_0) = -kt$.

The nature of the solvent markedly perturbs the stability of **2a**-Py. Compare $k = 5 \times 10^{-4}$ s^{-1}(5°C) in CH_3CN/Py ([Py] = 1 M), $k = 7 \times 10^{-3}$ s^{-1} (5°C) in Py and $k = 2 \times 10^{-3}$ s^{-1} (5°C) in H_2O/Py ([Py] = 1 M). Note that the rate constant of self-decay of activated bleomycin $k = 5.8 \times 10^{-3}$ s^{-1} (4°C) in H_2O [14] is rather close to that for the decay of **2a**-Py ($k = 2 \times 10^{-3}$ s^{-1}) at 5°C in H_2O/Py ([Py] = 1 M).

To elucidate the influence of the basicity of the sixth ligand B on the rate of the decay of **2a**-B, the following derivatives of Py with various pK_a values shown in brackets were used [38]: 3-Br-Py (2.84), Py (5.23), 3-Me-Py (5.68), 4-Me-Py (6.02) and 4-Me_2N-Py (9.58). Py and its derivatives were added into the aliquots of the same solution of **2a**-Py in CH_3CN (to make [B] = 1 M). The following rate constants were obtained at +20°C: 4×10^{-4} s^{-1} (3-Br-Py); 2×10^{-3} s^{-1}(Py); 2×10^{-3} s^{-1}(3-Me-Py); 2

$\times 10^{-3}$ s^{-1} (4-Me-Py); 6×10^{-3} s^{-1} (4-Me_2-N-Py). It is seen that with the increase of basicity of B, the rate constant of **2a**-B self-decay noticeably grows. The similar ''push effect'' of B was previously observed for heterolytic decay of acylperoxo iron(III) porphyrin complexes in CH_2Cl_2, that affords oxoferryl cation radical complexes $(Por^{+\cdot})Fe^{IV}=O$ [39].

The replacement of 2,2′-bipyridine ligands in **2a**-Py by 4,4′-dimethyl-2,2′-bipyridine ligands results in threefold increase of the rate constant of its decay at 20°C in CH_3CN/Py ([Py] = 1 M). This observation is in agreement with the reported data for acylperoxoiron(III) porphyrin complexes, where introduction of electron donating substituents at the meso position of the porphyrin ring accelerates the rate of their self-decay [39]. Unfortunately, in contrast to the iron porphyrin systems, we have no data on the structure of intermediates of the hydroperoxo complexes decomposition.

The hydroperoxo complex **2b**-Py with phenantroline ligands is less stable than the hydroperoxo complex **2a**-Py with bipyridine ligands. The rate constant of the **2b**-Py decomposition in CH_3CN/Py ([Py] = 1 M) at 20°C is 8×10^{-3} s^{-1} versus 2×10^{-3} s^{-1} for **2a**-Py in the same solvent and at the same temperature.

*3.4. Reactivity of the hydroperoxo complexes **2a**-B and **2b**-B*

To study the reactivity of the hydroperoxo complexes **2a**-Py and **2b**-Py, a substrate (cyclohexane, cyclohexene, methyl phenyl sulfide) was added to their solutions in Py or CH_3CN/Py ([Py] = 1 M) at −10°C to +20°C. The initial concentration of **2a**-Py or **2b**-Py was 2×10^{-4} to 5×10^{-4} M. It was found that the presence of listed substrates in solution (concentrations were up to 3 M) did not noticeably perturb the rate of self-decay of **2a**-Py and **2b**-Py. This rather unexpected result is consistent with the previous data obtained for activated bleomycin, where DNA also does not affect the rate of activated bleomycin self-decay [14]. Thus, **2a**-Py and **2b**-Py do not directly react with organic substrates and the observed decrease of the quasi steady-state concentration of **2a**-Py after the addition of cyclohexane into the catalytic system **1a**/HOOH/Py/AcOH (Fig. 4) is not caused by the increase of the rate of complex **2a**-Py decay (W_2), but by the decrease of the rate of its formation (W_1). It is still not entirely clear how cyclohexane can perturb W_1. If it is granted that free radicals ($OH^{\cdot}$, $HO_2^{\cdot}$) participate in formation of **2a**-Py, the possible way of reducing W_1 is the decrease of the concentration of free radicals in solution via their reaction with cyclohexane.

As a rule, alkylperoxo and hydroperoxo iron(III) intermediates were detected only at high excesses of oxidants (ROOH, HOOH), when a number of unidentified substrate-sensitive reactions could determine their concentrations. Thus, the attempts to derive data on the reactivity of LFe(OOH) or LFe(OOR) species from the drop of their quasi steady-state concentrations after the addition of a substrate to the reaction mixture [25,27,28] were inadequate.

The observed pseudo-first-order decrease of the concentration of $[Fe^{III}(TPA)(OO\,t\mathrm{Bu})(HOR)]^{2+}$ [18] can reflect the kinetics of the decomposition of excessive *t*BuOOH rather than the kinetics of the decay of the alkylperoxo intermediate, and thus the effect of cyclohexanol on this kinetics can not be connected with the reactivity of the alkylperoxo intermediate.

The only informative reactivity study of an hydroperoxo intermediate is the study of the activated bleomycin (Fe^{III}(BLM)(OOH)), which is believed to be responsible for the oxidative damage of DNA under aerobic conditions by Fe^{II}-BLM [14,15]. In contrast to the other mentioned intermediates, detected only at the excess of oxidants, activated bleomycin can be prepared via stoichiometric oxidation of Fe^{II}-BLM by dioxygen and thus kinetics of its self-decay can be reliably measured. As was mentioned, DNA did not affect the rate of activated bleomycin self-decay, however the rate of accumulation of DNA degradation products coin-

cided kinetically with the decay of activated bleomycin. The yield of oxidation products achieved 50% of the concentration of activated bleomycin decomposed [14]. This evidences in favour of the rate determining conversion of Fe^{III}(BLM)(OOH) to another active species prior to the reaction with substrate.

The results of this part of our study are the determination of the rates for self-decomposition processes of the complexes **2a**-Py, **2b**-Py and demonstration of the fact that organic substrates do not perturb these rates. These data allow evaluation of the upper limit for the rates of the reaction of **2a**-B or **2b**-B with organic substrates. The maximal values of these rates are not more than those of the rates of complexes **2a**-B or **2b**-B self-decomposition. In the opposite case, the addition of substrates would noticeably perturb the decay of these species. Secondly, the obtained data show that organic substrates can influence the steady-state concentration of the hydroperoxo and alkylperoxo iron(III) intermediates diminishing the rate of their formation rather than increasing the rate of their decay. This possibility should be taken into account in reactivity studies of peroxo iron species.

The main products of cyclohexane oxidation by the catalytic system **1a**/HOOH/Py/AcOH (the sample of Fig. 4) are cyclohexanone and cyclohexanol in 1:1 ratio. Catalyst:substrate ratio was 1:100 equiv., ketone and alcohol were formed in 4% yield each based on substrate. The oxidation of cyclohexene by this system affords products of allylic oxidation (cyclohexenone and cyclohexenol, their yields were 4% and 3%, respectively). This reactivity pattern is typical for oxidation by free radicals. The same oxidation products are observed for samples with reduced concentration of HOOH. It should be noted that the residual concentration of HOOH (10^{-2} M) was much larger than the concentration of **2a**-Py (10^{-4} M). The overall concentration of cyclohexane oxidation products in these samples was 3- to 10-fold larger than that of **2a**-Py. Thus, we cannot exclude that the Fenton decomposition of residual HOOH affords the major part of the products.

We have applied a spin-trapping technique for the characterization of transient free radicals in a solution containing complex **2a**-Py in CH_3CN. The 3,3,5,5-tetramethyl-1-pyrroline *N*-oxide (TMPO) purchased from Sigma was used as a spin trap. The nitrone spin traps DMPO and TMPO are widely used to provide evidence for the involvement of free radicals in many reactions in chemical and biological systems [40–42]. They are particularly useful for identifying oxygen-centered radicals, e.g. superoxide radical anion, peroxyl, alkoxyl and hydroxyl radicals. Similarly to all nitrones, TMPO captures short-living free radicals to give more stable nitroxyl radicals (spin adducts). The β-hydrogen hyperfine splitting constants (a_H) of spin adducts vary markedly with the nature of the radical trapped. Thus radicals can be recognized [40,41]. EPR spectrum recorded 3 min after the addition of TMPO (to make its concentration 0.1 M) to a sample containing **2a**-Py in CH_3CN at 20°C (Fig. 6a) is a superposition of the spectra of two adducts: $a_N = a_H = 14$ G and $a_N = 13$ G, $a_H = 6.5$ G with relative weights 1:2. The relative weight of the spectrum with $a_N = 13$ G, $a_H = 6.5$ G grows with time (Fig. 6b and c). According to hyperfine splitting constants the signal with $a_N = a_H = 14$ G belongs

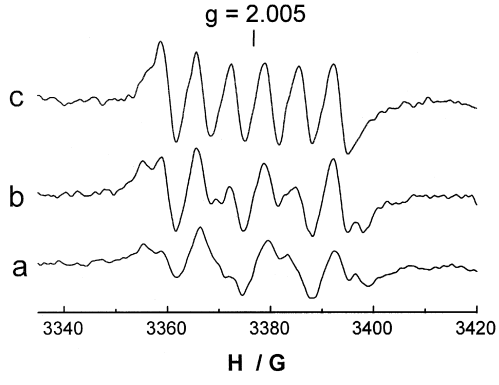

Fig. 6. X-band EPR spectra of TMPO spin adducts in a sample with reduced content of HOOH (ca. 10^{-2} M) containing $2 \cdot 10^{-4}$ M **2a**-Py in CH_3CN at various moments of time after addition of TMPO (to make its concentration 0.1 M) at 20°C: (a) 3 min, (b) 11 min, (c) 27 min.

to spin adduct TMPO/$^{\cdot}$OH. Formation of this adduct was observed for the catalytic system HOOH + $Co(acac)_2$ in CH_3CN [43]. In this system Fenton decomposition of hydrogen peroxide takes place. The EPR spectrum with $a_N = 13$ G, $a_H = 6.5$ G is characteristic for the adduct TMPO/$HO_2^{\cdot}$ [41]. Thus $^{\cdot}$OH and $HO_2^{\cdot}$ free radicals can be trapped in the solution of **2a**-Py in CH_3CN. Recently, $O_2^{-\cdot}/HO_2^{\cdot}$ free radicals were trapped in a water solution of activated bleomycin [35]. Note, that the attempts to trap free radicals directly in the catalytic system **1a**/HOOH/Py/AcOH were unsuccessful due to rapid decomposition of TMPO. Free tBuOO$^{\cdot}$ radicals can be directly observed in EPR spectra in the course of the reaction of **1a** with tBuOOH in CH_3CN. Their EPR spectrum in a frozen solution represents a sharp signal with axial anisotropy of g-factor, $g\| = 2.04$, $g_\perp = 2.008$ (Fig. 2c, the signal denoted by asterisks).

*3.5. Stability and reactivity of alkylperoxo complexes **3a**-B*

The alkylperoxo complex **3a**-CH_3CN obtained after extraction of tBuOOH from a reaction mixture rapidly disappears even at low temperatures with the following rate constants: $k = 10^{-3}$ $s^{-1}(-37°C)$; 2.5×10^{-3} $s^{-1}(-30°C)$; 5.8×10^{-3} $s^{-1}(-20°C)$; $E_a = 14 \pm 3$ kcal/mol. The rate constant of **3a**-MeOH self-decay in MeOH was found to be 2.4×10^{-3} s^{-1} at $-35°C$. The addition of Py or its derivatives ([B] = 1 M) to a solution of **3a**-CH_3CN in CH_3CN gives rise to its conversion to **3a**-B monitored by EPR. The rate constants for complexes **3a**-B decay in CH_3CN/B ([B] = 1 M) at $-30°C$ were as follows: 2.0×10^{-3} s^{-1} (3-Br-Py); 2.3×10^{-3} s^{-1}(Py); 3×10^{-3} s^{-1} (4-Me_2N-Py). It is seen that the basicity of the sixth ligand B only slightly perturbs the rates of decomposition of alkylperoxo species **3a**-B in contrast to hydroperoxo species **2a**-B (see Section 3.3). The similar small push effect was reported for homolytic decomposition of acylperoxoiron(III) porphyrin in toluene that affords oxoferryl complex (Por)$Fe^{IV} = O$ [39]. The alkylperoxo species are far less stable than corresponding hydroperoxo intermediates, $k = 1.2 \times 10^{-2}$ s^{-1} (**3a**-CH_3CN in CH_3CN at $-10°C$) and 2×10^{-4} s^{-1} (**2a**-Py in CH_3CN at $-10°C$). The different effect of axial ligation on the rate of self-decomposition of hydroperoxo (**2a**-B) and alkylperoxo (**3a**-B) species could provide evidence in favor of different mechanisms of their decay. However, we have still not obtained any additional support for this assumption.

The addition of cyclohexane, cyclohexene or methyl phenyl sulfide in concentrations up to 3 M to the reaction mixture does not perturb the rate of the complex **3a**-CH_3CN decomposition at $-25°C$. It indicates that **3a**-CH_3CN does not directly react with these organic substrates similarly to the hydroperoxo complexes **2a**-Py and **2b**-Py. GC analysis reveals mainly cyclohexanone and cyclohexanol in 1:1 ratio as the products of cyclohexane oxidation with solution of **3a**-CH_3CN in CH_3CN (obtained after extraction of tBuOOH) at $-20°C$. As the overall concentration of the products was not more than the initial concentration of **3a**-CH_3CN, its decomposition could produce an intermediate responsible for oxidation of the substrate. Based on 1:1 ratio of ketone to alcohol typical of free radical oxidation, this intermediate could be tBuO$^{\cdot}$ radicals. The catalytic system **1a**/tBuOOH/CH_3CN also oxidizes cyclohexane mainly into cyclohexanol and cyclohexanone in 1:1 ratio at 0°C. Probably, the reactive species of this oxidation are tBuO$^{\cdot}$(tBuO$_2^{\cdot}$) radicals formed in the course of tBuOOH decomposition. tBuO$_2^{\cdot}$ radicals at a concentration of ca. 10^{-5} M were observed in the catalytic system **1a**/tBuOOH/CH_3CN (Fig. 2c).

4. Conclusions

The first-order rate constants of self-decomposition of hydroperoxo and alkylperoxo com-

plexes $[Fe(bpy)_2(OOH)Py](NO_3)_2$ (**2a**-Py), $[Fe(phen)_2(OOH)Py](NO_3)_2$ (**2b**-Py) and $[Fe(bpy)_2(OOtBu)CH_3CN](NO_3)_2$ (**3a**-CH_3CN) were determined in the presence of various substrates and at various temperatures. The rate of decomposition of hydroperoxo complexes **2a**-B, where B are derivatives of Py (3-Br-Py, 3-Me-Py, 4-Me-Py and 4-Me_2N-Py) increases with the growth of basisity of B (push effect). Such an effect is markedly smaller for alkylperoxo species **3a**-B. ^{2}D NMR signals of *t*BuOO moieties of low-spin ferric alkylperoxo complexes **3a**-CH_3CN, **3a**-CH_3OH and **3a**-H_2O were detected for the first time. The addition of organic substrates (cyclohexane, cyclohexene, methyl phenyl sulfide) at a concentration up to 3 M at -10°C to $+20$°C does not noticeably change the rate of self-decomposition of **2a**-B, **2b**-Py and **3a**-B. Thus the intermediates concerned do not directly react with organic substrates. The reactivity patterns of **2a**-B, **2b**-Py and **3a**-B were characteristic for free radical oxidation. The determined rates of self-decomposition of complexes **2a**-B, **2b**-B and **3a**-B can be used for evaluation of the upper limit for their reactivity towards organic substrates.

To date there is an example [21], when a low-spin ferric hydroperoxo intermediate $[Fe(TPA)(OOH)]^{2+}$ detected in $[Fe(TPA)(CH_3CN)_2](ClO_4)_2/HOOH/CH_3CN$ system is believed to be responsible for epoxidation of 1-hexene that is typical for non radical oxidation. Further it would be interesting to study the influence of 1-hexene on the rate of $[Fe(TPA)(OOH)]^{2+}$ self-decay and to correlate the rate of this decay with the rate of epoxide formation to elucidate whether this hydroperoxo complex directly reacts with olefin or via formation of another reactive species.

Acknowledgements

This work was supported by Russian Fund of Basic Research, grant no.97-03-32495a and by Haldor Topse A/S.

References

[1] D.H.R. Barton, D. Doller, Acc. Chem. Res. 25 (1992) 504.
[2] D.H.R. Barton, S.D. Beviere, W. Chavasiri, E. Csuhai, D. Doller, W.-G. Liu, J. Am. Chem. Soc. 114 (1992) 2147.
[3] C. Shen, A. Sobkowiak, S. Jeon, D.T. Sawyer, J. Am. Chem. Soc. 112 (1990) 8212.
[4] S. Menage, J.-M. Vincent, C. Lambeaux, G. Chottard, A. Grand, M. Fontecave, Inorg. Chem. 32 (1993) 4766.
[5] R.A. Leising, J. Kim, M.A. Perez, L. Que, J. Am. Chem. Soc. 115 (1993) 9524.
[6] J. Kim, R.G. Harrison, Ch. Kim, L. Que, J. Am. Chem. Soc. 118 (1996) 4373.
[7] I.W.C.E. Arends, K.U. Ingold, D.D.M. Wayner, J. Am. Chem. Soc. 117 (1995) 4710.
[8] M. Newcomb, P.A. Simakov, S.-V. Park, Tetrahedron Lett. 37 (1996) 819.
[9] D.W. Snelgrove, A. MacFaul, K.U. Ingold, D.D.M. Wayner, Tetrahedron Lett. 37 (1996) 823.
[10] F. Minisci, F. Fontana, S. Aranco, F. Recupero, S. Banfi, S. Quici, J. Am. Chem. Soc. 117 (1995) 226.
[11] M. Selke, M.F. Sisemore, J.S. Valentine, J. Am. Chem. Soc. 118 (1996) 2008.
[12] F. Neese, E.L. Solomon, J. Am. Chem. Soc. 120 (1998) 12829.
[13] T.E. Westre, K.E. Leob, J.M. Zaletski, B. Hedman, K.O. Hodgson, E.I. Solomon, J. Am. Chem. Soc. 117 (1995) 1309.
[14] R.M. Burger, J. Peisach, S.B. Horwitz, J. Biol. Chem. 258 (1981) 11636.
[15] R.M. Burger, Chem. Rev. 98 (1998) 1153.
[16] J.W. Sam, X.-J. Tang, J. Peisach, J. Am. Chem. Soc. 116 (1994) 5250.
[17] S. Menage, E.C. Wilkinson, L. Que Jr., M. Fontecave, Angew. Chem., Int. Ed. Engl. 34 (1995) 203.
[18] J. Kim, E. Larka, E.C. Wilkinson, L. Que Jr., Angew. Chem., Int. Ed. Engl. 34 (1995) 2048.
[19] M. Lubben, A. Meetsma, E.C. Wilkinson, B. Feringa, L. Que Jr., Angew. Chem., Int. Ed. Engl. 34 (1995) 1512.
[20] M.E. de Vries, R.M. La Crois, G. Roelfes, H. Kooijman, A.L. Spek, R. Hage, B.L. Feringa, J. Chem. Soc., Chem. Commun. (1997) 1549.
[21] Ch. Kim, K. Chen, J. Kim, L. Que Jr., J. Am. Chem. Soc. 119 (1997) 5964.
[22] R.Y.N. Ho, G. Roelfes, B.L. Feringa, L. Que Jr., J. Am. Chem. Soc. 121 (1999) 264.
[23] K. Tajima, Inorg. Chim. Acta 163 (1989) 115.
[24] A. Sauer-Masarwa, N. Herron, C.M. Fendrick, D.H. Busch, Inorg. Chem. 32 (1993) 1086.
[25] K. Ah Lee, W. Nam, J. Am. Chem. Soc. 119 (1997) 1916.
[26] R.J. Guajardo, S.E. Hudson, S.J. Brown, P.K. Mascharak, J. Am. Chem. Soc. 115 (1993) 7971.
[27] C. Nguyen, R.J. Guajardo, P.K. Mascharak, Inorg. Chem. 35 (1996) 6273.
[28] A.P. Sobolev, D.E. Babushkin, E.P. Talsi, Mendeleev Commun. (1996) 33.
[29] N.A. Milas, D.M. Surgenor, J. Am. Chem. Soc. 68 (1946) 205.
[30] P.D. Bartlett, J.M. McBridge, J. Am. Chem. Soc. 87 (1965) 1727.

[31] S. Menage, J.M. Vincent, C. Lambeaux, G. Chottard, A. Grand, M. Fontecave, Inorg. Chem. 32 (1993) 4766.
[32] J.E. Plowman, T.M. Loehr, C.K. Schauer, O.P. Anderson, Inorg. Chem. 23 (1984) 3553.
[33] A.A. Shubin, G.M. Zhidomirov, Zh. Struct. Khim. 30 (1989) 67, (in Russian).
[34] S.C. Tang, S. Koch, G.C. Papaefthymion, S. Foner, R.B. Frankel, J.A. Ibers, R.H. Holm, J. Am. Chem. Soc. 98 (1976) 2414.
[35] Y. Sugiura, J. Am. Chem. Soc. 102 (1980) 5208.
[36] R.D. Arasasingham, A.L. Balch, Ch.R. Coruman, L. Latos-Gazinski, J. Am. Chem. Soc. 111 (1989) 4357.
[37] S. Uemura, A. Spencer, G. Wilkinson, J. Chem. Soc., Dalton Trans. 22 (1973) 2565.
[38] Comprehensive Heterocyclic Chemistry. The Structure, Reactions, Synthesis and Uses of Heterocyclic Compounds vol. 2 Pergamon, Oxford, 1986, Part 2A.
[39] K. Yamaguchi, Y. Watanabe, I. Morishima, J. Am. Chem. Soc. 115 (1993) 4058.
[40] E.G. Janzen, G.A. Evans, J. Liu, J. Magn. Reson. 9 (1973) 513.
[41] E.G. Janzen, R.V. Shetty, S.M. Kunanec, Can. J. Chem. 59 (1981) 756.
[42] P. Bilski, K. Reszka, M. Bilska, C.F. Chignell, J. Am. Chem. Soc. 118 (1996) 1330.
[43] E.P. Talsi, K.V. Shalyaev, J. Mol. Catal. 92 (1994) 245.